Ecotoxicology and Environmental Safety 302 (2025) 118683

Contents lists available at ScienceDirect

Ecotoxicology and Environmental Safety

journal homepage: www.elsevier.com/locate/ecoenv

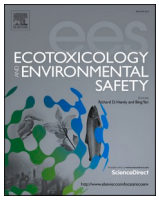

Polystyrene micro and nanoplastics: A comparative study of the cytotoxic effects exerted on *Mytilus galloprovincialis* gills

R. Romano [a,b], L. Rosati [c], G. Napolitano [a,b], F. Ferrigno [a], T. Chianese [c], C.M. Motta [c], P. Simoniello [a,*]

[a] Department of Science and Technology, University Parthenope, Napoli, Italy
[b] International PhD Programme, UNESCO Chair "Environment, Resources and Sustainable Development", Department of Science and Technology, Parthenope University of Naples, Naples 80143, Italy
[c] Department of Biology, University of Naples Federico II, Napoli, Italy

ARTICLE INFO

Keywords:
Cell stress
Goblet cells
Collagen deposition
Carbohydrate composition
Oxidative stress

ABSTRACT

Polystyrene microplastics (MP) and nanoplastics (NP) are significant contributors to the pollution of aquatic ecosystems. Their high persistence, small size, and high potential to enter food chains pose risks to humans and all living organisms. *Mytilus galloprovincialis* is a mussel native to the Mediterranean Sea, widely distributed in coastal environments. As a filter-feeder, it accumulates pollutants, making it a valuable bioindicator and model organism in environmental monitoring and research. In this work, we used adult mussels to evaluate the cytotoxic effects of polystyrene MP (5 μm) and NP (0.1 μm) on gill lamellae cyto-anatomy. The animals were exposed for 1, 3, and 11 days. Results showed increased reactive oxygen species (ROS), oxidative damage to lipids, and in vitro susceptibility to oxidants on day 3, as well as increased total antioxidant capacity on days 3 and 11. Parallel histological investigation demonstrated epithelial alterations from day 1, characterised by increased PCNA expression, particularly in the most exposed frontal epithelium. Marked alterations were also observed in the connective septa, where collagen deposition and disorganisation were detected. The activation of an immune response was evident by the increased presence of haemocytes and mucus cells. In all cases, the effects were more marked after exposure to NP. These results suggest a significant impairment of gill function, particularly in food collection, as the frontal and front lateral cilia were markedly affected. In conclusion, plastic reduction in the oceans is an issue that can no longer be postponed; the first step seems to be a more conscious use of this material.

1. Introduction

The over 335 million tons of plastic produced yearly have transformed the current historical period into the "Plastocene Epoch" (Avio et al., 2017). Discarded in all environments and degraded by physical, chemical, and biological factors (Wu et al., 2025), plastics have contaminated all natural matrices (Bergmann et al., 2019) and, above all, the seas (Eriksen et al., 2014).

Microplastics (MP; diameter < 5 mm) and nano plastics (NP; diameter < 1 μm) pose a threat since they are often mistaken for food by small aquatic organisms (Van Cauwenberghe et al., 2015). As a consequence, MP and NP are found in zooplanktonic species, including chaetognaths (Rodrigues et al., 2023), copepods (Fibbe et al., 2023), and salps (Johnston et al., 2023); in benthonic invertebrates (D'Costa, 2022; Krikech et al., 2023; Kovačić et al., 2024) and in vertebrates, from fish (Alberghini et al., 2022) to marine mammals (Merrill et al., 2023). Therefore, plastic particles have infiltrated all levels of the food chain, either through direct consumption or trophic transfer (Cverenkárová et al., 2021).

MP and NP negatively affect health, causing mechanical damage (Ali et al., 2024) and/or fasting (Shiu et al., 2022), or indirectly, by releasing toxic chemicals. Plastic can adsorb and carry pollutants present in the environment, such as heavy metals or persistent organic pollutants (La Nasa et al., 2021; Liu et al., 2022; Costigan et al., 2022). NP toxicity is particularly relevant since small particles can cross the cell membrane via energy-independent mechanisms or endocytosis. This may be clathrin- or caveolin-mediated or due to micropinocytosis (Liu et al., 2021), while MP can be internalised via phagocytosis (Ikuta et al., 2022).

* Corresponding author.
E-mail address: palma.simoniello@uniparthenope.it (P. Simoniello).

https://doi.org/10.1016/j.ecoenv.2025.118683
Received 24 March 2025; Received in revised form 9 July 2025; Accepted 11 July 2025
Available online 19 July 2025

Once inside cells, both MP and NP can induce the production of reactive oxygen species (ROS) through different mechanisms (Geremia et al., 2023). ROS production represents a molecular initiating event that can lead to cellular damage and alterations in cell functionality. ROS are very unstable and reactive by-products of cellular metabolism, comprising radical species, such as superoxide anion and hydroxyl radical, and non-radical species (H_2O_2) that can oxidatively damage biological molecules (lipids, proteins, and nucleic acids). The cellular antioxidant system can scavenge ROS in physiological conditions, preserving redox homeostasis. When ROS content overwhelms the antioxidant capacity, an oxidative stress condition is initiated (Napolitano et al., 2021).

Due to their characteristics, MP and NP pose a particularly severe threat to filter-feeding organisms, such as mussels. Mussels commonly live in shallow waters and prefer eutrophic areas near estuaries and large cities. The observed decline in mussel abundance is clear evidence of the harmful interference that anthropogenic activities exert on coastal biodiversity (Vaughn and Hoellein, 2018; Benjamin et al., 2022).

Understanding how organisms respond to plastic pollution is urgent; therefore, this comparative study investigated the histological and physiological effects of micro- and nano-polystyrene beads on the gills of *Mytilus galloprovincialis*. Polystyrene is commonly found in most everyday products and is one of the primary types of marine waste (Gonçalves et al., 2022).

M. galloprovincialis is the most common mussel in the Mediterranean Sea and an excellent model organism (Curpan et al., 2022; Habumugisha et al., 2024). In these animals, the gills also filter food particles, thereby exposing a large surface of contact and uptake of toxicants (Fogliano et al., 2023b). Exposure to MP (1×10^2 particles/mL) and NP (2.2×10^4 particles/mL) lasted 1, 3, or 11 days. The aim was to detect and compare early and late effects of MP and NP on gill lamellae. These effects were assessed using histological and physiological approaches to lay the foundation for in-depth biochemical and molecular studies.

2. Materials and methods

2.1. Animal care and treatments

Specimens of *Mytilus galloprovincialis* (valve range 6.60 ± 1.25 cm, n = 63/replicate experiment) were obtained from commercial sources in the reproductive period (December 2021 and March 2022; Rosati et al., 2019). Mussels were maintained in 100 L tanks with artificial seawater (Instant Ocean Sea Salt, salinity 38 ± 1 ‰) at 18 ± 1 °C under a natural light/dark photoperiod (10 h light/14 h dark) (Motta et al., 2018). They were fed marine zooplankton and phytoplankton for the aquarium (Seachem-Reef). An external pump connected to an oxygenator guaranteed oxygen levels and water circulation. No biological or chemical filter was used to prevent the absorption of MP and NP in the filtering materials. The animal's well-being was constantly monitored, and no mortality was recorded. No ethical protocol approval was necessary to work with this invertebrate species. Care was taken to minimise animal suffering and to reduce the use of unnecessary animals in the experimentation.

After 5 days of acclimation, mussels, in groups of 7, were randomly assigned to control, MP, or NP polycarbonate tanks (20 L/tank; 3 tanks/treatment; Motta et al., 2018). Exposures lasted for 1, 3 and 11 days. For the first two treatments, the water was left unchanged; for the latter, the water was changed on day 5. Polystyrene MP (5 μm; 1×10^7 particles/mL) and NP (0.1 μm; 1×10^9 particles/mL), purchased from Thermo Scientific™ (Duke Standards™ 2000 Series Uniform Polymer Particles), were diluted at final concentrations of 1×10^2 particles/mL (MP; Vroom et al., 2017) and 2.2×10^4 particles/mL (NP; Capolupo et al., 2021). The above-described experiment was conducted in triplicate (n = 63 animals per treatment).

2.2. Redox state evaluation

The gills (n = 3 animals/treatment) were dissected, pooled, weighed, and homogenised in 10 volumes of ice-cold 0.1 M potassium-phosphate buffer, pH 7.4, in a Potter-Elvehjem homogeniser set at a standard speed (500 rpm, 1 min). Protein content in the homogenate was determined using Bradford reagent according to the manufacturer's instructions (Bio-Rad, USA). Aliquots were used to determine ROS levels, oxidative damage to lipids (Hps), in vitro susceptibility to oxidants, and total antioxidant capacity (TAC). Measurements were performed in duplicate.

The ROS content was measured spectrofluorimetrically using a multimode microplate reader (Synergy™ HTX Multimode Microplate Reader, BioTek), with excitation and emission wavelengths of 485 and 530 nm, respectively. The method was carried out by following the ROS-induced conversion of 2',7'-dichlorodihydrofluorescin diacetate to dichlorofluorescein as per Driver et al. (Driver et al., 2000), with modifications (Napolitano et al., 2022). The ROS content was expressed as Relative Fluorescence Units (RFU)/μg protein.

Hps were determined spectrophotometrically according to Heath and Tappel (1976). The measures were obtained using a multimode microplate reader (Synergy™ HTX Multimode Microplate Reader, BioTek) set up at 340 nm, and Hps content was expressed as μmol NADPH oxidised/ min/mg protein.

Susceptibility to oxidative stress was determined by evaluating changes in hydroperoxide levels in homogenates treated with iron and ascorbate (10 min, room temperature; Napolitano et al., 2022). The reaction was stopped by adding 2, 6-di-t-butyl-p-cresol (BHT), and the hydroperoxide levels were evaluated according to Heath and Tappel (1976).

TAC was spectrophotometrically measured at 734 nm using a multimode microplate reader (Synergy™ HTX Mul-ti-Mode Microplate Reader, BioTek) according to Erel (Erel, 2004) with modifications (Napolitano et al., 2023). Total antioxidant capacity was expressed as BHT equivalent/ mg protein.

2.3. Histological analyses

Gill samples (n = 7/treatment) were collected at different exposure times, fixed in Bouin's (24 h), and embedded in paraffin according to standard protocols (Simoniello et al., 2010). Sections of 5 μm were stained with Galgano's trichrome or haemalum-eosin to show the general morphology (Motta et al., 2018) or with Picrosirius red to show collagen (Rosati et al., 2023). Slides were observed under bright and UV light. All images were acquired with a Zeiss Axiocam camera applied to a Zeiss Axioskop microscope (Zeiss, Jena, Germany).

Periodic acid-Schiff (PAS) staining highlighted mucin, glycogen, and glycoproteins (Motta et al., 2022). Positive cells were counted in 15 randomly taken digital photos (20x magnification). For each experimental group, at least 45 different lamellae were examined. A distinction was made between frontal and abfrontal epithelia.

Sugar residues were characterised by staining with FITC-conjugated lectins (Vector Laboratories Inc., Newark, CA, USA; 2 μl diluted in 50 μl PBS pH 7.4; Motta et al., 2022). Negative controls were prepared by omitting the lectin (to check for tissue autofluorescence) or co-incubating the slides with the lectin and the specific competing sugar, to check for lectin binding specificity. Two independent observers assessed labelling intensity (Thaer and Sernetz, 2012). Lectins used were DBA (*Dolichos biflorus* agglutinin) for N-acetyl-galactosamine (galNAc) and PNA (*Arachis hypogaea* agglutinin) for terminal galactose (gal) (Fogliano et al., 2023b). Images were acquired with Nikon Eclipse E200 and Nikon Eclipse Ni-U.

2.4. Immunohistochemistry

Sections mounted on polylysine glass slides were treated with 10 mM citrate buffer pH 6.0 to unmask antigens and incubated in 2.5 % H_2O_2 in

methanol to block endogenous peroxidase (Verderame et al., 2022). Non-specific signals were reduced by incubation in normal goat serum (Pierce, Rockford, IL, USA) for 1 h at room temperature. Slides were incubated overnight at 4 °C with a primary rabbit anti-human PCNA antibody (Elabscience, Bionovation Inc., Rome, IT), diluted 1:300 in normal goat serum. The next day, the sections were incubated with HRP-conjugated goat-anti-rabbit secondary antibody diluted 1:200 in normal goat serum for 1 h at room temperature and with avidin-biotin-peroxidase complex (ABC immune peroxidase kit, Pierce) for another 1 h at room temperature. Finally, the sections were stained with diaminobenzidine as chromogen and counterstained with Meyer's haematoxylin. Negative controls were obtained by omitting incubation with the primary antibody. The reaction was observed with a Zeiss Axioskop microscope, and images were acquired using the Nikon Eclipse Ni-U microscope and Nikon DS-*Fi*3 camera.

Positive cell nuclei were counted in 35 randomly taken digital photos (20x magnification). For each experimental group, at least 50 different lamellae were examined. A distinction was made among frontal, respiratory and abfrontal epithelia.

2.5. Western Blot

Western Blot validated the specificity of the PCNA antibody. Gills (n = 3) were homogenised at 4 °C in 5 mL of RIPA buffer (50 mM Tris-HCl pH 7.4, 150 mM NaCl, 1 mM EDTA, 10 % NP-40, and protease inhibitor cocktail). The homogenates were centrifuged at 7000 g for 10 min at 4 °C, and recovered proteins were quantified using the PIERCE method. Fifty µg of proteins were run on 13 % SDS/polyacrylamide gels at 60 mA and stained with Coomassie Blue R-250 (Rosati et al., 2017). After electrophoresis, the proteins were transferred to a nitrocellulose membrane at 350 mA for 1 h. The membrane was double blocked at room temperature, before with 7 % powdered milk dissolved in TBS 1x-Tween for 45 min and after with 7 % BSA in TBS-Tween for 45 min. Then, the membrane was incubated overnight at 4 °C with the PCNA antibody diluted in TBS-Tween + 2 % milk at 4 °C. On the second day, the membrane was washed in TBS-Tween buffer and incubated for 1 h with peroxidase-conjugated anti-rabbit IgG secondary antibody (Santa Cruz, Sc-2005) diluted 1: 2000 in TBS-T and 2.5 % milk powder. Finally, to detect the bands, the membranes were incubated with DAB as chromogen (Roche, 11718096001).

2.6. Data collection and analysis

Redox biomarker data were reported as means ± SEM of three experiments (n = 3). Absorbance from skeletal rods stained with Picrosirius red was determined in high-resolution digital photos (400 dpi;

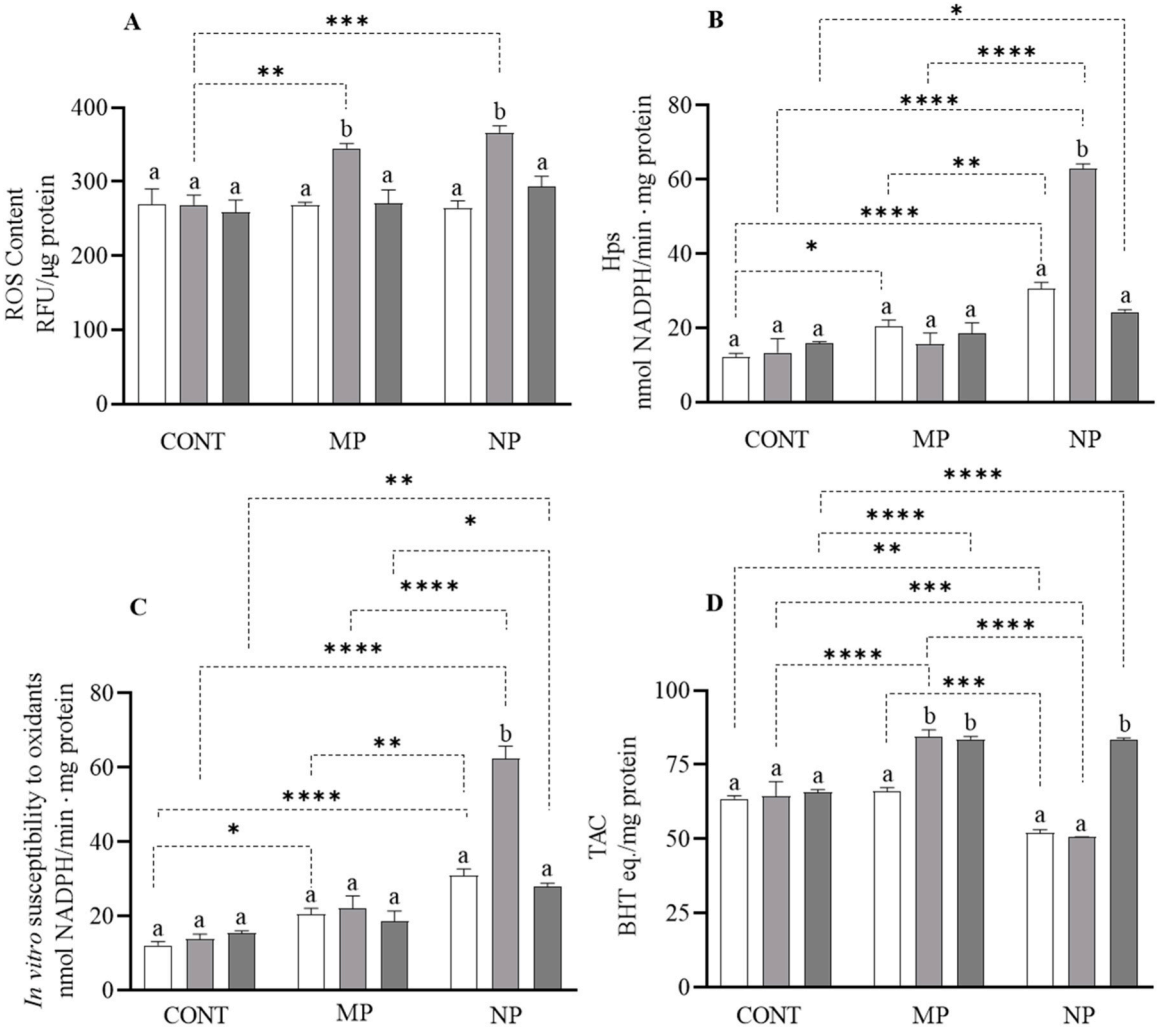

Fig. 1. ROS content (A), oxidative damage to lipids, Hps (B), *in vitro* susceptibility to oxidants (C), and total antioxidant capacities, TAC (D) in gills' homogenates from *Mytilus galloprovincialis* exposed to MP or NP for 1, 3, or 11 days. Data are mean values ± SD of 3 experiments (n = 3). Significance was assessed using two-way ANOVA followed by a Tukey post hoc test. Different letters indicate statistically significant differences within the same experimental group; $p < 0.05$. Asterisks indicate significant differences among groups; *, $p < 0.05$; **$p < 0.01$; ***$p < 0.001$; ****$p < 0.0001$. CONT: control, MP: microplastics, NP: nanoplastics.

n = 25/treatment) transformed into 8-bit, 256 grayscale TIFF images. These were examined using the ImageJ program (free version 1.8.0; last updated 22 May 2023). Optical density (grayscale) was determined in n = 85 areas/treatment (see yellow rectangle in Fig. 3F for area size). Data were expressed as a per cent of control values using the following formula: data from treatment/data from control *100 (Fogliano et al., 2024).

GraphPad Prism software version 9 (GraphPad Software Inc., San Diego, CA, USA) was employed for statistical analysis. A two-way analysis of variance, followed by a Tukey post-hoc test, was conducted. The minimum p-value accepted as significant was $p < 0.05$.

3. Results

3.1. Redox state of gill lamellae

ROS content (Fig. 1A), constant in 1-, 3-, and 11-day control animals, significantly increased on day 3 in animals exposed to MP ($p < 0.01$) or NP ($p < 0.001$) and returned to control values by day 11.

Hps level (Fig. 1B) and *in vitro* susceptibility to oxidants (Fig. 1C), constant in control animals, significantly increased on day 1 ($p < 0.05$) in animals exposed to MP, returning to control values on days 3 and 11. In contrast, in animals exposed to NP, values increased significantly, reaching a peak on day 3 ($p < 0.0001$). They were consistently higher than values registered in the respective controls and MP-exposed lamellae.

Total antioxidant capacities (Fig. 1D) did not change in control animals and animals exposed to MP for 1 day. On days 3 and 11, in contrast, values were significantly higher ($p < 0.0001$). NP exposure caused a significant decrease in TAC on days 1 ($p < 0.01$) and 3 ($p < 0.001$) and an increase on day 11 ($p < 0.0001$). Values on days 1 and 3 were significantly lower ($p < 0.001$ and $p < 0.0001$) than those recorded after MP exposure.

3.2. Interference of MP and NP on gill morphology

Control lamellae showed regular epithelia sustained by a connective skeletal rod (Fig. 2A). In the front lateral area, the cells were cylindrical and characterised by the presence of long cilia (Fig. 2A). These water pumps were sustained by basal bodies that made cell cytoplasm intensely eosinophilic and autofluorescent (Fig. 2B). In the intermediate area, the epithelium was composed of cuboidal respiratory cells (Fig. 2A). In contrast, in the abfrontal epithelia, cells returned cylindrical and intercalated with occasional secretory cells, rich in intensely eosinophilic, autofluorescent granules (Fig. 2B).

After exposure to MP, time-dependent morphological alterations appeared. The most evident was the increased number of secretory cells (Fig. 2C-E) in the abfrontal epithelium and the appearance of melanin-rich cells in the respiratory epithelium (Fig. 2F). In the frontal epithelium, ciliary damage was observed, and correspondingly, the cytoplasm appeared less intensely stained by eosin (Fig. 2D, E).

In specimens exposed to NP, the frontal epithelium was regularly

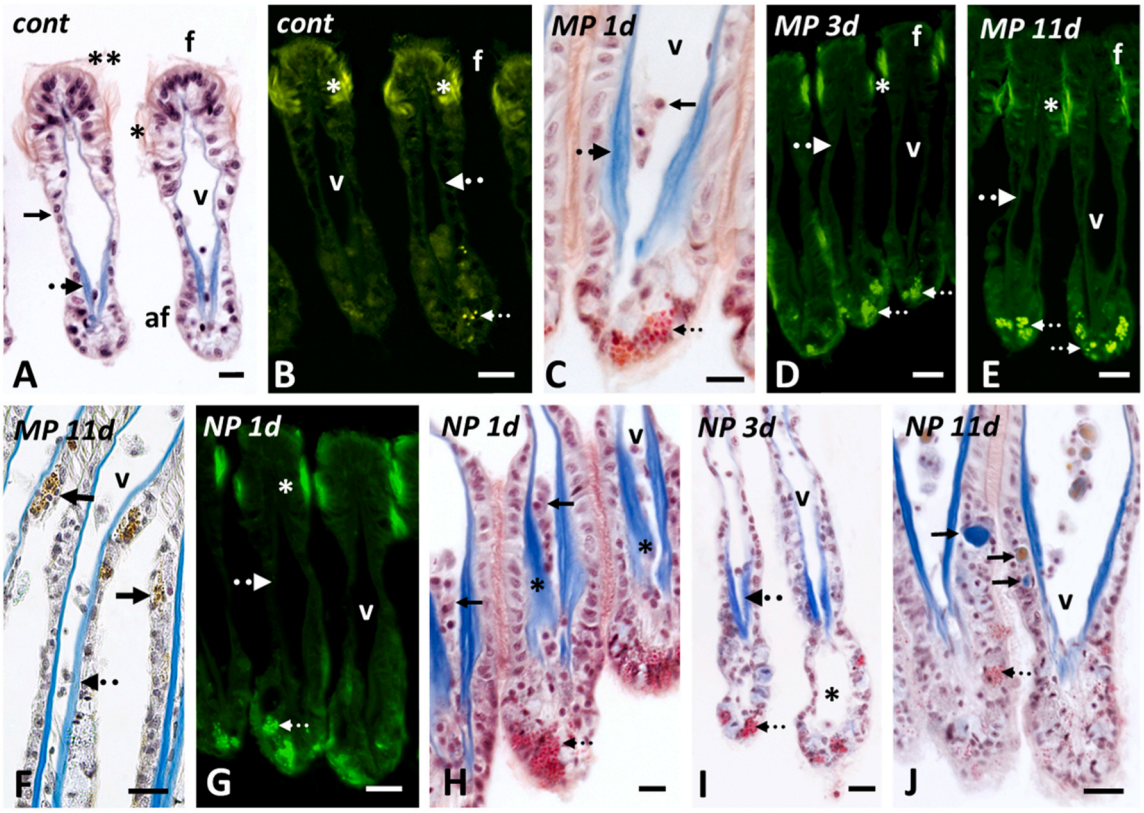

Fig. 2. Gill morphology in *Mytilus galloprovincialis* exposed to MP or NP for 1, 3, or 11 days. A) General anatomy of the lamellae showing the frontal (f) and abfrontal (af) areas. Hemolymph vessel (v), skeletal rod (dotted arrow), frontal (**) and fronto-lateral (*) cilia. B) Autofluorescent ciliated cells (*) and occasional secretory cells (dotted small arrow). Skeletal rod (dotted arrow). C) Abfrontal (af) zone. Skeletal rod (dotted arrow), lobed hemocytes (dotted small arrow) in vessel (v), secretory cells (small arrow). D-E) Poorly autofluorescent ciliated cells (*) and increased number of secretory cells (small arrows). Skeletal rod (dotted arrow) and vessel (v). F) Respiratory epithelium with melanin-rich cells (arrows). Skeletal rod (dotted arrow). G) Reduced autofluorescence in ciliated cells (*). Secretory cells (small arrow), skeletal rod (dotted arrow), and vessel (v). H) Abfrontal zone; epithelium rich in secretory cells (dotted small arrow). Hemocytes (small arrows) in vessels. (v). Notice the irregular skeletal rod (*). I) Abfrontal zone showing degraded areas (*). J) Abfrontal epithelium with infiltrated hemocytes (arrows). Secretory cells (small arrow). cont: control, MP: microplastics, NP: nanoplastics. Galgano's staining observed under bright fields (A, C, F, H-J) or UV light to show eosin autofluorescence (B, D-E, G). Scale bars: 15 μm; C and I, 10 μm.

organised (data not shown); however, cilia were shorter, and cytoplasm autofluorescence was reduced (Fig. 2G). The abfrontal zone showed marked alterations: it was often enriched in secretory cells (Fig. 2H), infiltrated with several haemocytes (Fig. 2H) and occasionally disorganised (Fig. 2I). Respiratory epithelium showed several melanin-rich cells (data not shown).

3.3. Effects of MP and NP on skeletal rod collagen

In control lamellae, the rods appeared as a continuous plate, delimiting the central hemolymph vessel. The frontal and lateral portions were thin (Fig. 3A), with a relatively homogeneous density (Fig. 3B). In the abfrontal portion, rods were thicker (Fig. 3A) and less homogeneous (Fig. 3C), especially distally, where they were often also irregular in shape (Fig. 3C).

No matter the exposure time, the skeletal rods of lamellae exposed to MP appeared regular (Fig. 3D), similar to the skeletal rods of control animals. Under UV light, however, the frontal portion often seemed loose (Fig. 3E), while the density of the abfrontal portion was irregular. Occasional epithelial cells were moderately stained (Fig. 3F).

In animals exposed to NP, dose-dependent alterations were observed. In the frontal zone, after 1 day of exposure, thickened rods and several intensely stained epithelial cells were already observed (Fig. 3G-H). In the abfrontal zone, the skeletal rods were thick and very irregular in shape and density, often completely disorganised distally (Fig. 3G, I). Several epithelial cells were stained (Fig. 3I). At 11 days, the frontal portion of the rods was often asymmetrically stained (Fig. 3J, K), while, in the abfrontal zone, the rods were inhomogeneous and lacked the distal portion (Fig. 3J, L).

The optical density analysis (Fig. 3M) confirmed the loss of collagen observed in histological sections. No differences were observed in the control samples, so values were pooled (Fig. 3M); in contrast, MP

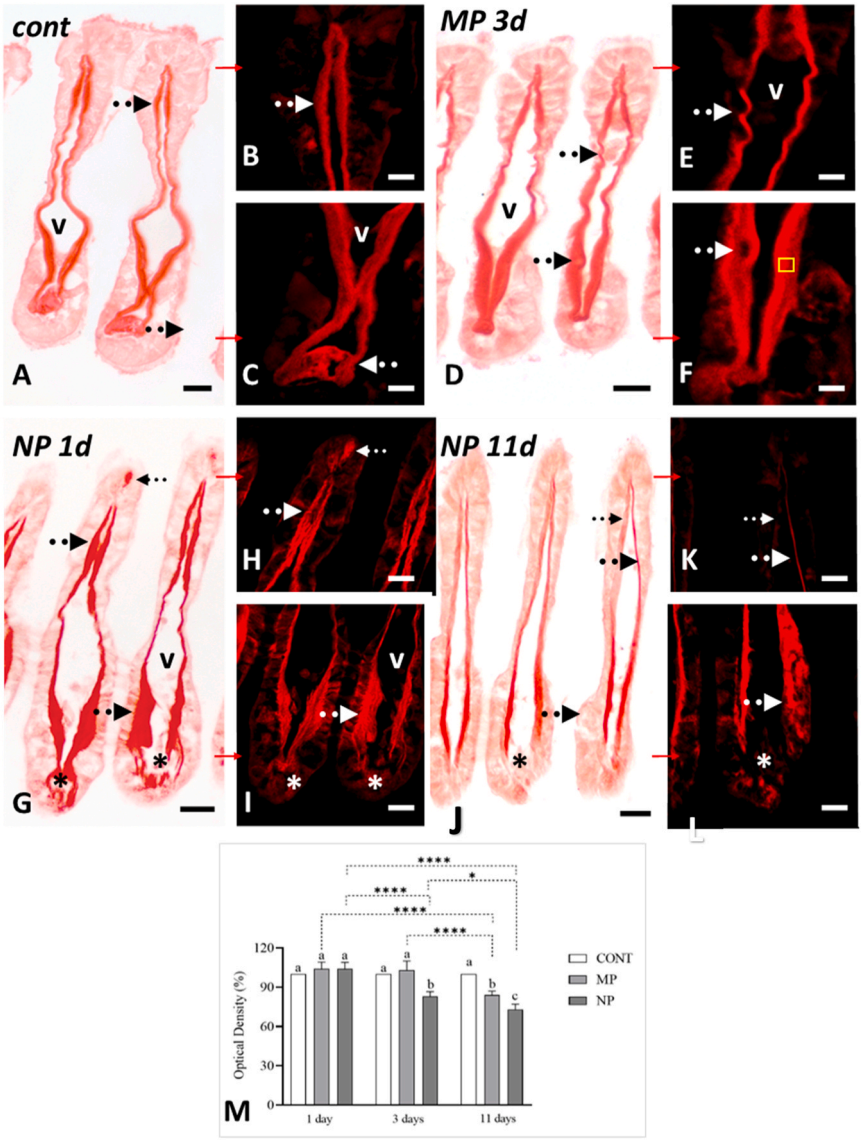

Fig. 3. Collagen in gill skeletal rods of *Mytilus galloprovincialis* exposed to MP or NP for 1, 3 or 11 days. A, D, G, J) Stained skeletal rod (dotted arrows) lining the lymph vessel (v). Details of frontal (B, E, H, K) and abfrontal (C, F, I, L) rods. Notice the occasional stained epithelial cells (dotted small arrows; fig. G, H), the abnormal rods (*, fig. G, I and J, L), and the asymmetrically stained frontal rod (dotted small arrows, fig. J, K). Picrosirius Red staining observed under a bright field (white background pictures) or UV light (black background pictures). cont: control, MP: microplastics, NP: nanoplastics. Scare bars: 15 μm. M) Decrease in optical density (grey values) in abfrontal skeletal rods. Measures (n = 85/treatment) were obtained in areas such as that shown by the yellow square in Figure F. Values were expressed as per cent of controls. Different letters indicate significant differences with respect to the corresponding control; $p < 0.05$. Asterisks indicate significant differences among groups; *, $p < 0.05$; ****$p < 0.0001$.

exposure caused a 16 % decrease in absorbance on day 11 ($p < 0.0001$). The effects of NP exposure were particularly significant ($p < 0.0001$) since optical density decreased by 17 % on day 3 and dropped by 27 % on day 11.

3.4. Effect of MP and NP on carbohydrates

3.4.1. Staining with PAS

In controls, PAS stained an average of 3.3 ± 0.6 frontal (Figs. 4A, J) and 2.0 ± 0.6 abfrontal (Fig. 4A, B, J) goblet cells and the skeletal rod (Fig. 4A, B). No differences were appreciated at different experimental times (data not shown) so data were pooled (Fig. 4J). After exposure to MP, on days 1 and 3, the number of goblet cells showed no variation in the frontal epithelium (Fig. 4C, D, J), while it increased in the abfrontal epithelium ($p < 0.05$, Fig. 4E), reaching an average of 6.7 ± 0.5 cells (Fig. 4J). On day 11, the number of goblet cells in both epithelia was significantly higher (4.9 ± 0.4 and 5.4 ± 0.3, respectively; $p < 0.05$) than the respective controls (Fig. 4J).

Exposure to NP significantly increased the goblet cell number (Fig. 4J). In frontal epithelia, on days 1 and 3, the average number was 4.4 cells; on day 11, the value rose to 5.3 ± 0.5. In the abfrontal epithelium, cells increased in number on day 1 (7.2 ± 0.7), then reduced to 3.9 and 4.6 cells on days 3 and 11, respectively.

3.4.2. Staining with fluorescent lectins PNA and DBA

In controls, the skeletal rod was intensely stained by PNA, indicating the presence of abundant galactose (Fig. 5A, B). In lamellae exposed to MP (Fig. 5C) or NP (Fig. 5D), no labeling was detected in rods and epithelia, no matter the experimental time. Occasional labeled secretory cells were observed in the abfrontal epithelia of control lamellae (Fig. 5B) or lamellae exposed to NP (Fig. 5D).

In control lamellae, staining with lectin DBA demonstrated that the skeletal rod contained abundant galNAc (Fig. 5E). No matter the experimental time, labeling disappeared from lamellae exposed to MP (Fig. 5F) but not from those exposed to NP (Fig. 5G). Secretory cells were unstained (Fig. 5G).

3.5. Proliferating cell nuclear antigen detection by immunocytochemistry

PCNA antibody specificity was first validated by Western blot assay

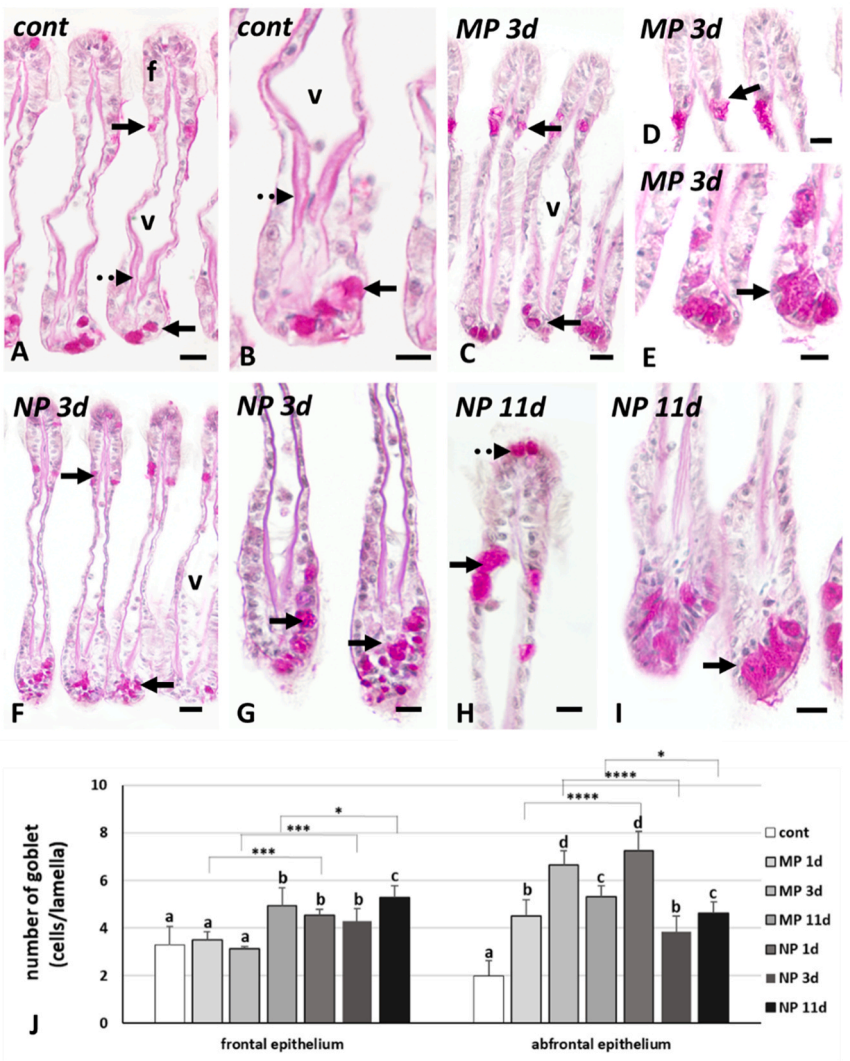

Fig. 4. PAS staining of *Mytilus galloprovincialis* gills exposed to MP or NP for 1, 3, or 11 days. A-B). Stained goblet cells (arrows) and skeletal rods (dotted arrows). Vessels (v). C and F) Lamellae with stained goblet cells (arrows). Details of frontal (fig. D, H) and abfrontal (fig. E, G, and I) zones. cont: control, MP: microplastics, NP: nanoplastics. Scale bars: 15 μm. J) Variations in the number of PAS-positive cells; frontal and abfrontal epithelia (n = 45 lamellae/treatment). Different letters indicate significant differences with respect to controls; $p < 0.05$. Asterisks indicate significant differences between MP and NP; *$p < 0.05$; ***$p < 0.001$; ****$p < 0.0001$.

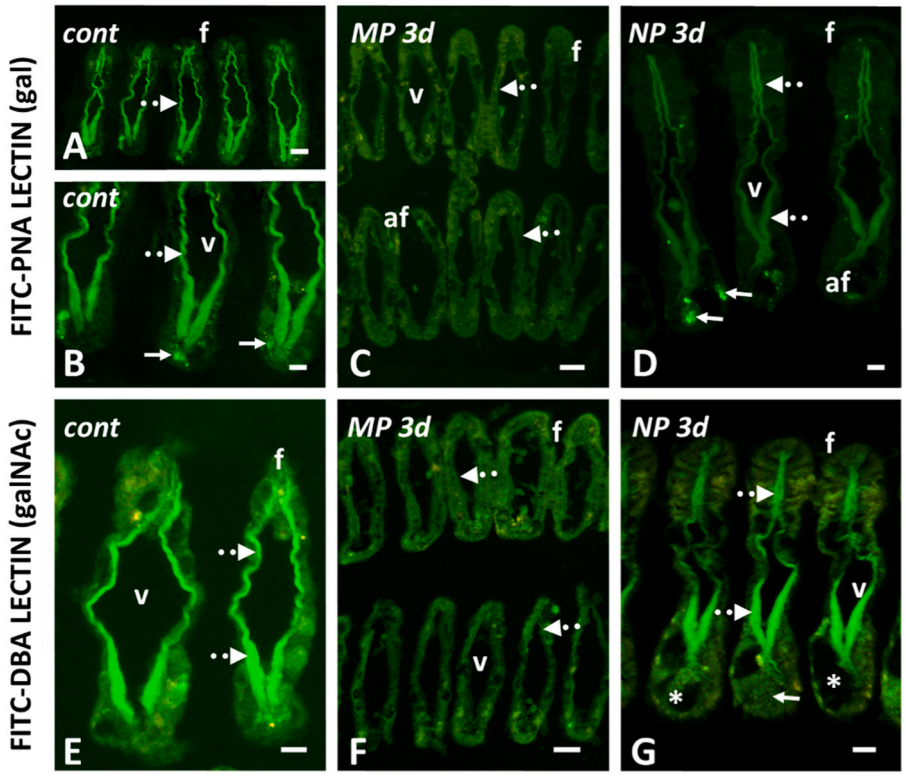

Fig. 5. Carbohydrate characterisation in gills lamellae of *M. galloprovincialis* exposed to MP or NP for 1, 3, or 11 days. A) Labeled skeletal rod (dotted arrow) lining the lymph vessel (v). B) Detail of the abfrontal zone. Notice the labeled secretory cells (small arrows). C) Unlabeled lamellae and rods (dotted arrows). D) Unlabeled lamellae and rods (dotted arrows) but labeled secretory cells in abfrontal epithelia (small arrows). E and G) Labeled skeletal rod (dotted arrows) and unlabeled secretory cells (small arrow). Large unlabeled areas (*). F) Unlabeled rods (dotted arrows). Frontal zone (f), abfrontal zone (af), vessel (v). FITC-conjugated lectin staining observed under UV light. cont: control, MP: microplastics, NP: nanoplastics. Scale bars: A, C, F, 30 μm; B, D, E, G, 15 μm.

on mussel gill protein extracts. Results showed a single band of about 34 kDa (Fig. 6A).

In control animals, immunohistochemistry demonstrated that labeled nuclei were rare in frontal, respiratory and abfrontal epithelia. Counts indicated an average of 0.2, 0.1 and 0.7 nuclei per lamella, respectively (Fig. 6B, G) and no changes occurred during the experiments (data not shown). After exposure to MP, positive nuclei increased in number. The average raised to 0.9 nuclei per lamella in frontal (Fig. 6C, G) and abfrontal (Fig. 6D, G) epithelia and 0.6 nuclei per lamella in the respiratory epithelia.

After NP exposure, positive nuclei increased significantly ($p < 0.05$), and marked differences were observed in different epithelia. In the frontal zone, the average number of labeled nuclei rose from 4.5 ± 0.1, on day 1, to a maximum of 7.1 ± 0.4 on day 11 (Fig. 6E, G). In the respiratory epithelia, the number also increased but less dramatically, reaching a maximum of 1.9 ± 0.1 nuclei per lamella on day 11 (Fig. 6G). In the abfrontal epithelium, the average number significantly decreased on day 1 ($p < 0.05$, 0.2 nuclei per lamella), increased on day 3, with 1.2 ± 0.2 labeled nuclei per lamella (Fig. 6F, G), and decreased on day 11.

4. Discussion

Given their constant contact with the external environment and dual function in respiration and filter feeding, gills are a primary target for environmental pollutants. In our investigation, exposure to polystyrene led to significant oxidative stress and damage to the lamellae. Such effects could depend on the release from micro/nanobeads of toxic compounds, particularly volatile organic compounds (Yamashita et al., 2009; Iizuka et al., 2020), which, by dissolving in lipids, interfere with the cell membranes of epithelial cells (Sikkema et al., 1995; Salimi et al., 2017). In additionally, it cannot be excluded that MP and NP released toxic styrene (Wang et al., 2023).

The oxidative damage to the lipids due to ROS is already evident in samples observed after one day of exposure to both MP and NP, confirming these compounds' high permeability and toxicity. The effect was more pronounced in samples exposed to the NP. This is likely due to the higher surface area-to-volume ratio of microspheres and the fact that their number was two orders of magnitude greater than that of MP. As a result, it is expected that NP will release more adsorbed chemicals. (Brown et al., 2001; Collin-Faure et al., 2022; Nardi et al., 2024). The relationship, however, is not so direct, and many factors contribute (Gulizia et al., 2023).

Relevant damage was observed in most exposed tissues, particularly at the cilia level, in the frontal epithelia. Due to their position and structure, they offer a large surface area and absorption capacity for toxic compounds released by polystyrene. Abnormalities in ciliary structure significantly impair pump function, impacting feeding and leading to energy problems. The consequences on water circulation would also lead to a hypoxic condition, especially in mid and long-term exposures, with severe implications for animal health.

As demonstrated in moulds (Yue et al., 2023), volatile organic compounds disrupt cell membrane integrity, allowing pathogens to leak into the cells. In mussels, contact with the apical membranes of gill epithelial cells might have increased the bioavailability of volatile compounds (Sikkema et al., 1995) and favoured the entry of polystyrene beads. This hypothesis, however, needs to be verified. Although preliminary tests indicate that toxic benzaldehyde and styrene are released form polystyrene in significant concentrations (Iizuka et al., 2020; Wang et al., 2023; Motta et al., 2024), light microscopy did not reveal the presence of MP adhering to the epithelial surface or into the cells at any experimental time. The numerous washes required for sample processing can account for the absence of adhering particles. In contrast, the

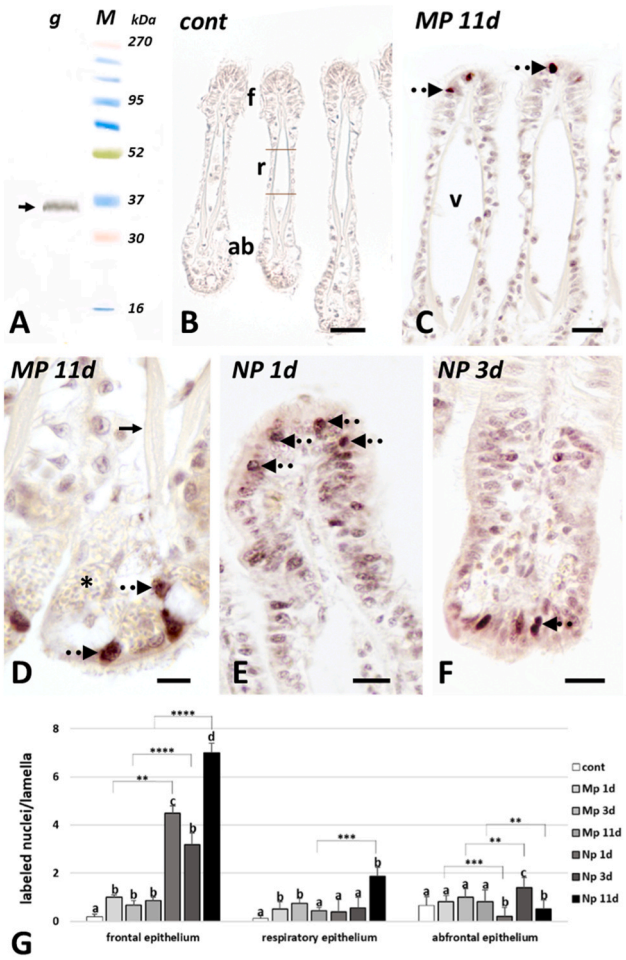

Fig. 6. PCNA-positive nuclei in gill epithelia of *Mytilus galloprovincialis* exposed to MP or NP for 1, 3, or 11 days. A) Western blot of gill protein extract (in lane g); the antibody detects a single band at about 34 kDa. M: protein ladder. B) Absence of stained cells in frontal (f), respiratory (r), and abfrontal (ab) epithelia. C and E) Stained nuclei in the frontal epithelium (dotted arrows). Haemolymph vessel (v). D and F) Stained nuclei in the abfrontal epithelium (dotted arrows). Unstained skeletal rod (arrow) and secretory cell (*). cont: control, MP: microplastics, NP: nanoplastics. Scale bars: B, 50 μm; C, E, F, 15 μm; D, 10 μm. G) Average number of labeled nuclei in frontal, respiratory, and abfrontal epithelia. Different letters indicate statistically significant differences with respect to the control; $p < 0.05$. Asterisks indicate significant differences between the MP and NP groups; **$p < 0.01$; ***$p < 0.001$; ****$p < 0.0001$; $n = 50$ lamellae/treatment.

absence of MP inside the epithelial cells remains unexplained, as epithelial cells are susceptible to phagocytosis and can store bacteria (Tame et al., 2022). For NP, which enters mussel gill epithelial cells via phagocytosis (Ikuta et al., 2022), detection was impossible due to the resolution limits of the light microscope. The uptaken particles would remain enclosed in membrane-delimited vacuoles, accumulating in cells, and interfering in cellular processes (Huffman Ringwood, 2021). This evidence is not entirely consistent with the fact that volatile compounds disturb plasma membrane organisation (Sikkema et al., 1995). Therefore, TEM investigations are necessary to clarify the destiny of internalised particles.

Another indication of the stressed condition of lamellar epithelia was the hyperplasia of goblet cells, a prompt defence mechanism of the mucosa (Garcia-Reyero et al., 2015), activated by toxicants (Motta et al., 2018; Fogliano et al., 2023a), including polystyrene beads (De Marco et al., 2023). It should be noted, however, that the increased number of cells was not associated with a significant increase in mucus released. Mucus production and mucus release are separate steps, controlled by different neural, mechanical, biochemical, and environmental signals (Hutchinson et al., 2007).

The composition of the lamellar epithelium also changed due to the increased number of other cell types, first of all, of the hemocytes that infiltrated the abfrontal epithelium, especially after NP exposure. This was expected because polystyrene induces inflammation and immunological responses (Wu et al., 2022; Cao et al., 2023; Del Piano et al., 2023). The moderate increase suggests a prompt recovery once the insult stops (de de de Oliveira David et al., 2008). In addition, in the respiratory and abfrontal epithelium, there was a notable increase in secretory cells, rich in eosinophilic protein granules, with high affinity for PAS and lectins PNA and DBA (Hidalgo et al., 1987). As suggested in the fish gill lamellae, they would contribute to mucus elaborations (Amores et al., 1984). Finally, in the respiratory epithelium, exposure to polystyrene caused an increase in cells rich in melanin granules (Quezada-Rodriguez et al., 2023). Together with hemocyte infiltration, these cells' presence confirms the tissue's inflammatory condition (De Vico and Carella, 2012).

Interestingly, oxidative stress biomarkers suggest that both micro- and nanobeads activate time-dependent tissue adaptation processes. The increase in ROS production induced by 3 and 11 days of exposure to MPs was not associated with an increase in oxidative damage to lipids or in *vitro* susceptibility to oxidants. However, the increase in the total antioxidant capacity of the gills after 3 days of exposure, which was maintained even after 11 days, may explain the observed containment of oxidative damage and *in vitro* susceptibility to oxidants. On the contrary, gill tissue requires longer to adapt to NP exposure. Three days of exposure induced an increase in ROS production not associated with an increase in the antioxidant defence system, resulting in a marked increase in the level of Hps and *in vitro* susceptibility to oxidants. On the contrary, the total antioxidant capacity of the gill tissue was significantly increased after an 11-day exposure to NP, resulting in a consequent reduction in the Hps level and susceptibility to oxidants. These results suggested that lamellar tissue is resilient to polystyrene exposure and can recover from damage. While it is true that ROS activate the antioxidant defence system as signal molecules (Napolitano et al., 2021), they are particularly reactive molecules that cause a cascade of degenerative effects, such as genotoxic effects (Avio et al., 2015) and DNA damage (Barzilai and Yamamoto, 2004). In our experiments, PCNA expression increased markedly in lamellar epithelia, indicating that damage had occurred since DNA repair mechanisms were activated (Paunesku et al., 2001). The lack of necrosis or apoptosis suggests that lamellar integrity and functionality were maintained. Mortality, in effect, was not registered.

Staining with Picrosirius red demonstrated that MP and NP interfered with the skeletal rod, particularly with collagen deposition in the abfrontal zone. The observed alterations may be correlated with the demonstrated ability of polystyrene surfaces to activate fibroblasts *in vitro* so to facilitate the formation of fibrillar collagen (Elliott et al., 2008). A contribution of oxidative stress should also be postulated (Martins et al., 2021).

The cytological analyses showed disorganisation and density reduction, especially in samples exposed to NP, since day 3 of exposure. The rods line the haemolymph vessels, so interferences in controlling gas diffusion and O_2 and CO_2 balance should be postulated (Fogliano et al., 2023b). Reduced density, in contrast, may have favoured hemocyte invasion and, consequently, the inflammatory response and the innate defence (Venier et al., 2011).

Collagen is not the only rod component altered by polystyrene exposure. The skeletal rod also contains chitin, a target of toxicants due to its high content of positively charged glucosamine residues (Einsporn and Koehler, 2008). Polystyrene binds to chitin through non-covalent bonding and physical adhesion, mediated by hydrophobic and van der Waals forces (Liu et al., 2021). The analysis with lectins indicated that MP reduced galNAC and galactose residues. Unfortunately, no data on

carbohydrate rod composition in mussels could be found in the literature. Therefore, at present, it is challenging to formulate hypotheses regarding the consequences of altering the rods carbohydrate composition (interference with gas exchange, support to the epithelium or onset of local inflammation). Nor is there a justification for why the same effect was not observed in samples exposed to NP.

In conclusion, our results indicated that polystyrene induces oxidative damage, affecting the lamellar structure: the epithelial cells are altered, and DNA repair is activated. The increased number of secreting and goblet cells supports an inflammatory condition, and the altered collagen in rods suggests an impaired functionality of the entire structure, including feeding. The experiments also indicated that NP is faster and more effective than MP in inducing damage and that the tissues can respond efficiently to restore tissue integrity.

Mussels, as filter-feeding species, have a long history of adapting to compounds dissolved in water. Therefore, it is not surprising that their gills have adapted to cope with the insult represented by polystyrene. However, this does not mean mussels can tolerate prolonged and intense exposures. To reduce plastic contamination is therefore essential for preserving this ecologically significant component of coastal marine environments.

Funding

This work was supported by the Ministero dell'Istruzione, dell'Università e della Ricerca [grant numbers 20204YRYS5_006; Finanziamento dele attività di base di ricerca (FFABR) MIUR art.1, comma 295, Legge 11/12/2016 n 232.

CRediT authorship contribution statement

Rossana Romano: Methodology, Formal analysis, Investigation, Data Curation, Writing – original draft, Writing – review & editing. **Luigi Rosati:** Investigation, Visualization, Data curation, Writing – original draft, Writing – review & editing, Funding acquisition. **Gaetana Napolitano:** Methodology, Writing – original draft, Writing – review & editing, Data Curation, Investigation. **Federica Ferrigno:** Resources, Methodology, Writing – review & editing. **Teresa Chianese:** Methodology. **Chiara Maria Motta:** Supervision, Funding acquisition, Visualization, Resources, Writing – original draft, Writing – review & editing. **Palma Simoniello:** Conceptualization, Methodology, Investigation, Data curation, Resources, Validation, Formal analysis, Supervision, Visualization, Writing – original draft, Writing – review & editing, Funding acquisition.

Declaration of Competing Interest

The authors declare that they have no known competing financial interests or personal relationships that could have appeared to influence the work reported in this paper.

Data availability

Data will be made available on request.

References

Alberghini, L., Truant, A., Santonicola, S., Colavita, G., Giaccone, V., 2022. Microplastics in fish and fishery products and risks for human health: a review. Int. J. Environ. Res. Public Health 20 (1), 789. https://doi.org/10.3390/ijerph20010789.

Ali, N., Katsouli, J., Marczylo, E.L., Gant, T.W., Wright, S., de la Serna, J.B., 2024. The potential impacts of micro-and-nano plastics on various organ systems in humans. EBioMedicine 99. https://doi.org/10.1016/j.ebiom.2023.104901.

Amores, P., Hidalgo, J., Navas, P., Sanchez-Aguayo, I., JL, L.C., 1984. Cellular types in the gill arch of the teleost *Cyprinus carpio* (Cyprinidae, Pisces). A histochemical and ultrastructural study. Basic Appl. Histochem. 28 (3), 291–307.

Avio, C.G., Gorbi, S., Milan, M., Benedetti, M., Fattorini, D., d'Errico, G., Pauletto, M., Bargelloni, L., Regoli, F., 2015. Pollutant bioavailability and toxicological risk from microplastics to marine mussels. Environ. Pollut. 198, 211–222. https://doi.org/10.1016/j.envpol.2014.12.021.

Avio, C.G., Gorbi, S., Regoli, F., 2017. Plastics and microplastics in the oceans: from emerging pollutants to emerged threat. Mar. Environ. Res. 128, 2–11. https://doi.org/10.1016/j.marenvres.2016.05.012.

Barzilai, A., Yamamoto, K.I., 2004. DNA damage responses to oxidative stress. DNA Repair 3 (8-9), 1109–1115. https://doi.org/10.1016/j.dnarep.2004.03.002.

Benjamin, E.D., Handley, S.J., Hale, R., Toone, T.A., Jeffs, A., Hillman, J.R., 2022. Biodiversity associated with restored small-scale mussel habitats has restoration decision implications. Biodivers. Conserv. 31, 2833–2855. https://doi.org/10.1007/s10531-022-02462-1.

Bergmann, M., Mützel, S., Primpke, S., Tekman, M.B., Trachsel, J., Gerdts, G., 2019. White and wonderful? Microplastics prevail in snow from the Alps to the Arctic. Sci. Adv. 5 (8), eaax1157. https://doi.org/10.1126/sciadv.aax1157.

Brown, D.M., Wilson, M.R., MacNee, W., Stone, V., Donaldson, K., 2001. Size-dependent proinflammatory effects of ultrafine polystyrene particles: a role for surface area and oxidative stress in the enhanced activity of ultra fines. Toxicol. Appl. Pharmacol. 175 (3), 191–199. https://doi.org/10.1006/taap.2001.9240.

Cao, J., Xu, R., Wang, F., Geng, Y., Xu, T., Zhu, M., Lv, H., Xu, S., Guo, M.Y., 2023. Polyethylene microplastics trigger cell apoptosis and inflammation via oxidative stress and activation of the NLRP3 inflammasome in carp gills. Fish. Shellfish Immunol. 132, 108470. https://doi.org/10.1016/j.fsi.2022.108470.

Capolupo, M., Valbonesi, P., Fabbri, E., 2021. A comparative assessment of the chronic effects of micro-and nano-plastics on the physiology of the Mediterranean mussel *Mytilus galloprovincialis*. Nanomaterials 11 (3), 649. https://doi.org/10.3390/nano11030649.

Collin-Faure, V., Dalzon, B., Devcic, J., Diemer, H., Cianférani, S., Rabilloud, T., 2022. Does size matter? A proteomics-informed comparison of the effects of polystyrene beads of different sizes on macrophages. Environmental Science Nano 9 (8), 2827–2840. https://doi.org/10.1039/D2EN00214K.

Costigan, E., Collins, A., Hatinoglu, M.D., Bhagat, K., MacRae, J., Perreault, F., Apul, O., 2022. Adsorption of organic pollutants by microplastics: overview of a dissonant literature. J. Hazard. Mater. Adv. 6, 100091. https://doi.org/10.1016/j.hazadv.2022.100091.

Curpan, A.S., Impellitteri, F., Plavan, G., Ciobica, A., Faggio, C., 2022. *Mytilus galloprovincialis*: an essential, low-cost model organism for the impact of xenobiotics on oxidative stress and public health. Comparative Biochemistry Physiology Part C Toxicology Pharmacology 256, 109302. https://doi.org/10.1016/j.cbpc.2022.109302.

Cverenkárová, K., Valachovičová, M., Mackuľak, T., Žemlička, L., Bírošová, L., 2021. Microplastics in the food chain. Life 11 (12), 1349. https://doi.org/10.3390/life11121349.

D'Costa, A.H., 2022. Microplastics in decapod crustaceans: accumulation, toxicity and impacts, a review. Sci. Total Environ. 832, 154963. https://doi.org/10.1016/j.scitotenv.2022.154963.

De Marco, G., Eliso, M.C., Oliveri Conti, G., Galati, M., Billè, B., Maisano, M., Ferrante, M., Cappello, T., 2023. Short-term exposure to polystyrene microplastics hampers the cellular function of gills in the Mediterranean mussel *Mytilus galloprovincialis*. Aquat. Toxicol. 264 (2023), 106736. https://doi.org/10.1016/j.aquatox.2023.106736.

De Vico, G., Carella, F., 2012. Morphological features of the inflammatory response in molluscs. Res. Vet. Sci. 93 (3), 1109–1115. https://doi.org/10.1016/j.rvsc.2012.03.014.

Del Piano, F., Lama, A., Piccolo, G., Addeo, N.F., Iaccarino, D., Fusco, G., Riccio, L., De Biase, D., Mattace Raso, G., Meli, R., Ferrante, M.C., 2023. Impact of polystyrene microplastic exposure on gilthead seabream (*Sparus aurata* L, 1758): differential inflammatory and immune response between anterior and posterior intestine. Sci. Total Environ. 879, 163201. https://doi.org/10.1016/j.scitotenv.2023.163201.

Driver, A.S., Kodavanti, P.R., Mundy, W.R., 2000. Age-related changes in reactive oxygen species production in rat brain homogenates. Neurotoxicology Teratol. 22 (2), 175–181. https://doi.org/10.1016/s0892-0362(99)00069-0.

Einsporn, S., Koehler, A., 2008. Immuno-localisations (GSSP) of subcellular accumulation sites of phenanthrene, aroclor 1254 and lead (Pb) in relation to cytopathologies in the gills and digestive gland of the mussel *Mytilus edulis*. Mar. Environ. Res. 66 (1), 185–186. https://doi.org/10.1016/j.marenvres.2008.02.053.

Elliott, J.T., Halter, M., Plant, A.L., Woodward, J.T., Langenbach, K.J., Tona, A., 2008. Evaluating the performance of fibrillar collagen films formed at polystyrene surfaces as cell culture substrates. Biointerphases 3 (2), 19–28.

Erel, O., 2004. A novel automated direct measurement method for total antioxidant capacity using a new generation, more stable ABTS radical cation. Clin. Biochem 37 (4), 277–285. https://doi.org/10.1016/j.clinbiochem.2003.11.015.

Eriksen, M., Lebreton, L.C., Carson, H.S., Thiel, M., Moore, C.J., Borerro, J.C., Galgani, F., Ryan, P.G., Reisser, J., 2014. Plastic pollution in the world's oceans: more than 5 trillion plastic pieces weighing over 250,000 tons afloat at sea. PloS One 9 (12), e111913. https://doi.org/10.1371/journal.pone.0111913.

Fibbe, M.C., Carroll, D., Gowans, S., Siuda, A.N., 2023. Ingestion of microplastics by copepods in Tampa Bay Estuary, FL. Front. Ecol. Evol. 11, 1143377. https://doi.org/10.3389/fevo.2023.1143377.

Fogliano, C., Carotenuto, R., Panzuto, R., Spennato, V., De Bonis, S., Simoniello, P., Raggio, A., Avallone, B., Agnisola, C., Motta, C.M., 2023a. Behavioral alterations and gills damage in *Mytilus galloprovincialis* exposed to an environmental concentration of delorazepam. Environ. Toxicol. Pharmacol. 97, 104030. https://doi.org/10.1016/j.etap.2022.104030.

Fogliano, C., Carotenuto, R., Agnisola, C., Simoniello, P., Karam, M., Manfredonia, C., Avallone, B., Motta, C.M., 2023b. Benzodiazepine delorazepam induces locomotory hyperactivity and alterations in pedal mucus texture in the freshwater gastropod

Planorbarius corneus. Int. J. Mol. Sci. 24 (23), 17070. https://doi.org/10.3390/ijms242317070.
Fogliano, C., Carotenuto, R., Agnisola, C., Motta, C.M., Avallone, B., 2024. Impact of benzodiazepine delorazepam on growth and behaviour of *Artemia salina* Nauplii. Biology 13 (10), 808. https://doi.org/10.3390/biology13100808.
Garcia-Reyero, N., Thornton, C., Hawkins, A.D., Escalon, L., Kennedy, A.J., Steevens, J. A., Willett, K.L., 2015. Assessing the exposure to nanosilver and silver nitrate on fathead minnow gill gene expression and mucus production. Environ. Nanotechnol. Monit. Manag. 4, 58–66. https://doi.org/10.1016/j.enmm.2015.06.001.
Geremia, E., Muscari Tomajoli, M.T., Murano, C., Petito, A., Fasciolo, G., 2023. The impact of micro- and nanoplastics on aquatic organisms: mechanisms of oxidative stress and implications for human health. A review. Environments 10 (9), 161. https://doi.org/10.3390/environments10090161.
Gulizia, A.M., Patel, K., Philippa, B., Motti, C.A., van Herwerden, L., Vamvounis, G., 2023. Understanding plasticiser leaching from polystyrene microplastics. Sci. Total Environ. 857, 159099.
Habumugisha, T., Zhang, Z., Uwizewe, C., Yan, C., Ndayishimiye, J.C., Rehman, A., Zhang, X., 2024. Toxicological review of micro- and nano-plastics in aquatic environments: Risks to ecosystems, food web dynamics and human health. Ecotoxicol. Environ. Saf. 278, 116426. https://doi.org/10.1016/j.ecoenv.2024.116426.
Heath, R.L., Tappel, A.L., 1976. A new sensitive assay for the measurement of hydroperoxides. Anal. Biochem. 76 (1), 184–191. https://doi.org/10.1016/0003-2697(76)90277-3.
Hidalgo, J., Velasco, A., Sanchez Aguayo, I., Amores, P., 1987. Light microscopic characterization of glycoconjugates in secretory cells of the carp (*Cyprinus carpio*) gill epithelium. Histochemistry 88, 65–73. https://doi.org/10.1007/BF00490170.
Huffman Ringwood, A., 2021. Bivalves as biological sieves: bioreactivity pathways of microplastics and nanoplastics. Biol. Bull. 241 (2), 185–195. https://doi.org/10.1086/716259.
Hutchinson, N., Davies, M.S., Ng, J.S., Williams, G.A., 2007. Trail following behaviour in relation to pedal mucus production in the intertidal gastropod *Monodonta labio* (Linnaeus). J. Exp. Mar. Biol. Ecol. 349 (2), 313–322.
Iizuka, A., Mizukoshi, A., Noguchi, M., Yamasaki, A., 2020. Emission fluxes of styrene monomers and other chemicals for products containing expanded polystyrene beads. Plos One 15 (10), e0239458. https://doi.org/10.1371/journal.pone.0239458.
Ikuta, T., Tame, A., Takahashi, T., Nomaki, H., Nakajima, R., 2022. Microplastic particles are phagocytosed in gill cells of deep-sea and coastal mussels. Front. Mar. Sci. 9, 1034950. https://doi.org/10.3389/fmars.2022.1034950.
Johnston, L.W., Bergami, E., Rowlands, E., Manno, C., 2023. Organic or junk food? Microplastic contamination in Antarctic krill and salps. R. Soc. Open Sci. 10 (3) https://doi.org/10.1098%2Frsos.221421.
Kovačić, I., Štefanko, K., Špada, V., Pustijanac, E., Buršić, M., Burić, P., 2024. Microplastics in Mediterranean Mussel *Mytilus galloprovincialis*: comparison between cultured and wildtype mussels from the Northern Adriatic. Appl. Sci. 14 (5), 2056. https://doi.org/10.3390/app14052056.
Krikech, I., Conti, G.O., Pulvirenti, E., Rapisarda, P., Castrogiovanni, M., Maisano, M., Gaël Le Pennec, D., Leermakers, M., Ferrante, M., Cappello, T., Ezziyyani, M., 2023. Microplastics ($\leq$ 10 μm) bioaccumulation in marine sponges along the Moroccan Mediterranean coast: insights into species-specific distribution and potential bioindication. Environ. Res. 235, 116608. https://doi.org/10.1016/j.envres.2023.116608.
La Nasa, J., Lomonaco, T., Manco, E., Ceccarini, A., Fuoco, R., Corti, A., Modugno, F., Castelvetro, V., Degano, I., 2021. Plastic breeze: volatile organic compounds (VOCs) emitted by degrading macro-and microplastics analysed by selected ion flow-tube mass spectrometry. Chemosphere 270, 128612. https://doi.org/10.1016/j.chemosphere.2020.128612.
Liu, L., Xu, K., Zhang, B., Ye, Y., Zhang, Q., Jiang, W., 2021. Cellular internalization and release of polystyrene microplastics and nanoplastics. Sci. Total Environ. 779, 146523. https://doi.org/10.1016/j.scitotenv.2021.146523.
Liu, S., Huang, J., Zhang, W., Shi, L., Yi, K., Yu, H., Zhang, C., Li, S., Li, J., 2022. Microplastics as a vehicle of heavy metals in aquatic environments: A review of adsorption factors, mechanisms, and biological effects. J. Environ. Manag. 302, 113995. https://doi.org/10.1016/j.jenvman.2021.113995.
Martins, S.G., Zilhão, R., Thorsteinsdóttir, S., Carlos, A.R., 2021. Linking oxidative stress and DNA damage to changes in the expression of extracellular matrix components. Front. Genet. 12, 673002. https://doi.org/10.3389/fgene.2021.673002.
Merrill, G.B., Hermabessiere, L., Rochman, C.M., Nowacek, D.P., 2023. Microplastics in marine mammal blubber, melon, and other tissues: evidence of translocation. Environ. Pollut. 335, 122252. https://doi.org/10.1016/j.envpol.2023.122252.
Motta, C.M., Tizzano, M., Tagliafierro, A.M., Simoniello, P., Panzuto, R., Esposito, L., Migliaccio, V., Rosati, L., Avallone, B., 2018. Biocide triclosan impairs byssus formation in marine mussels *Mytilus galloprovincialis*. Environ. Pollut. 241, 388–396. https://doi.org/10.1016/j.envpol.2018.05.064.
Motta, C.M., Califano, E., Scudiero, R., Avallone, B., Fogliano, C., De Bonis, S., Raggio, A., Simoniello, P., 2022. Effects of cadmium exposure on gut villi in *Danio rerio*. Int. J. Mol. Sci. 23 (4), 1927. https://doi.org/10.3390/ijms23041927.
Motta, C.M., Trifuoggi, M., Toscanesi, M., Fasciolo, G., Venditti, P., Fogliano, C., Raggio, A., Avallone, B., Carotenuto, R., 2024. Polystyrene microbeads release volatile compounds: effect on *Artemia salina* early development. Eur. J. Histochem. 68, 21, 21. ISSN 1121-760X.
Napolitano, G., Fasciolo, G., Venditti, P., 2021. Mitochondrial management of reactive oxygen species. Antioxidants 10 (11), 1824. https://doi.org/10.3390/antiox10111824.
Napolitano, G., Fasciolo, G., Magnacca, N., Goglia, F., Lombardi, A., Venditti, P., 2022. Oxidative damage and mitochondrial functionality in hearts from KO UCP3 mice housed at thermoneutrality. J. Physiol. Biochem. 78 (2), 415–425. https://doi.org/10.1007/s13105-022-00882-9.
Napolitano, G., Capriello, T., Venditti, P., Fasciolo, G., La Pietra, A., Trifuoggi, M., Giarra, A., Agnisola, C., Ferrandino, I., 2023. Aluminum induces a stress response in zebrafish gills by influencing metabolic parameters, morphology, and redox homeostasis. Comparative Biochemistry Physiology. Toxicology pharmacology CBP 271, 109633. https://doi.org/10.1016/j.cbpc.2023.109633.
Nardi, A., Pittura, L., d'Errico, G., Cesaroni, D., Mongera, F., Gorbi, S., Benedetti, M., Regoli, F., 2024. Cellular effects of microplastics are influenced by their dimension: mechanistic relationships and integrated criteria for particles definition. Environ. Pollut. 344, 123327. https://doi.org/10.1016/j.envpol.2024.123327.
de Oliveira David, J.A., Salaroli, R.B., Fontanetti, C.S., 2008. The significance of changes in *Mytella falcata* (Orbigny, 1842) gill filaments chronically exposed to polluted environments. Micron 39 (8), 1293–1299. https://doi.org/10.1016/j.micron.2008.03.001.
Paunesku, T., Mittal, S., Protić, M., Oryhon, J., Korolev, S.V., Joachimiak, A., Woloschak, G.E., 2001. Proliferating cell nuclear antigen (PCNA): ringmaster of the genome. Int. J. Radiat. Biol. 77 (10), 1007–1021. https://doi.org/10.1080/09553000110069335.
Quezada-Rodriguez, P.R., Taylor, R.S., Jantawongsri, K., Nowak, B.F., Wynne, J.W., 2023. Association between melanin deposits in gill tissue and microbiome across different hatchery-reared Atlantic salmon. J. Appl. Microbiol. 134 (2), lxac073. https://doi.org/10.1093/jambio/lxac073.
Rodrigues, S.M., Espincho, F., Elliott, M., Almeida, C.M.R., Ramos, S., 2023. Methodology optimization to quantify microplastic presence in planktonic copepods, chaetognaths and fish larvae. MethodsX 11, 102466. https://doi.org/10.1016/j.mex.2023.102466.
Rosati, L., Santillo, A., Di Fiore, M.M., Andreuccetti, P., Prisco, M., 2017. Testicular steroidogenic enzymes in the lizard Podarcis sicula during the spermatogenic cycle. C. R. Biol. 340 (11-12), 492–498. https://doi.org/10.1016/j.crvi.2017.10.001.
Rosati, L., Agnese, M., Abagnale, L., Aniello, F., Andreuccetti, P., Prisco, M., 2019. The mussel *Mytilus galloprovincialis* in the Bay of Naples: new insights on oogenic cycle and its hormonal control. Anat. Rec. 302 (6), 1039–1049. https://doi.org/10.1002/ar.24075.
Rosati, L., Chianese, T., De Gregorio, V., Verderame, M., Raggio, A., Motta, C.M., Scudiero, R., 2023. Glyphosate interference in follicular organization in the wall lizard *Podarcis siculus*. Int. J. Mol. Sci. 24 (8), 7363. https://doi.org/10.3390/ijms24087363.
Salimi, A., Talatappe, B.S., Pourahmad, J., 2017. Xylene induces oxidative stress and mitochondrial damage in isolated human lymphocytes. Toxicol. Res. 33, 233–238. https://doi.org/10.5487/TR.2017.33.3.233.
Shiu, H.T., Pan, X., Liu, Q., Long, K., Cheng, K.K.Y., Ko, B.C.B., Fang, J.K.-H., Zhu, Y., 2022. Dietary exposure to polystyrene nanoplastics impairs fasting-induced lipolysis in adipose tissue from high-fat diet-fed mice. J. Hazard. Mater. 440, 129698. https://doi.org/10.1016/j.jhazmat.2022.129698.
Sikkema, J.A.N., de Bont, J.A., Poolman, B., 1995. Mechanisms of membrane toxicity of hydrocarbons. Microbiol. Rev. 59 (2), 201–222. https://doi.org/10.1128/mr.59.2.201-222.1995.
Simoniello, P., Filosa, S., Riggio, M., Scudiero, R., Tammaro, S., Trinchella, F., Motta, C. M., 2010. Responses to cadmium intoxication in the liver of the wall lizard Podarcis sicula. Comp. Biochem. Physiol. C Toxicol. Pharmacol. 151 (2), 194–203. https://doi.org/10.1016/j.cbpc.2009.10.005.
Tame, A., Maruyama, T., Yoshida, T., 2022. Phagocytosis of exogenous bacteria by gill epithelial cells in the deep-sea symbiotic mussel *Bathymodiolus japonicus*. R. Soc. Open Sci. 9 (5), 211384. https://doi.org/10.1098/rsos.211384.
Thaer, A.A., Sernetz, M. (Eds.), 2012. Fluorescence techniques in cell biology. Springer Science & Business Media.
Van Cauwenberghe, L., Devriese, L., Galgani, F., Robbens, J., Janssen, C.R., 2015. Microplastics in sediments: a review of techniques, occurrence and effects. Mar. Environ. Res. 111, 5–17. https://doi.org/10.1016/j.marenvres.2015.06.007.
Vaughn, C.C., Hoellein, T.J., 2018. Bivalve impacts in freshwater and marine ecosystems. Annu. Rev. Ecol. Evol. Syst. 49 (1), 183–208. https://doi.org/10.1146/annurev-ecolsys-110617-062703.
Venier, P., Varotto, L., Rosani, U., Millino, C., Celegato, B., Bernante, F., Lanfranchi, G., Novoa, B., Roch, P., Figueras, A., Pallavicini, A., 2011. Insights into the innate immunity of the Mediterranean mussel *Mytilus galloprovincialis*. BMC Genom. 12, 1–19. https://doi.org/10.1186/1471-2164-12-69.
Verderame, M., Chianese, T., Rosati, L., Scudiero, R., 2022. Molecular and histological effects of glyphosate on testicular tissue of the lizard *Podarcis siculus*. Int. J. Mol. Sci. 23 (9), 4850. https://doi.org/10.3390/ijms23094850.
Vroom, R.J., Koelmans, A.A., Besseling, E., Halsband, C., 2017. Aging of microplastics promotes their ingestion by marine zooplankton. Environ. Pollut. 231, 987–996. https://doi.org/10.1016/j.envpol.2017.08.088.
Wang, J., Lee, J., Kwon, E.E., Jeong, S., 2023. Quantitative analysis of polystyrene microplastic and styrene monomer released from plastic food containers. Heliyon 9 (5). https://doi.org/10.1016/j.heliyon.2023.e15787.
Wu, Baihui, Yu, Haiyang, Lei, Pengyu, He, Jiaxuan, Yi, Jia, Wu, Wei, Wang, Hanbing, Yang, Qinsi, Zeng, Guoming, Sun, Da, 2025. Microplastics in aquatic ecosystems: Detection, source tracing, and sustainable management strategies. Ecotoxicol. Environ. Saf. 291, 117883. https://doi.org/10.1016/j.ecoenv.2025.117883.

Wu, H., Guo, J., Yao, Y., Xu, S., 2022. Polystyrene nanoplastics induced cardiomyocyte apoptosis and myocardial inflammation in carp by promoting ROS production. Fish. Shellfish Immunol. 125 (2022), 1–8. https://doi.org/10.1016/j.fsi.2022.04.048.

Yamashita, K., Yamamoto, N., Mizukoshi, A., Noguchi, M., Ni, Y., Yanagisawa, Y., 2009. Compositions of volatile organic compounds emitted from melted virgin and waste plastic pellets. J. Air Waste Manag. Assoc. 59 (3), 273–278. https://doi.org/10.3155/1047-3289.59.3.273.

Yue, Y., Wang, Z., Zhong, T., Guo, M., Huang, L., Yang, L., Kan, J., Zalán, Z., Hegyi, F., Takács, K., Du, M., 2023. Antifungal mechanisms of volatile organic compounds produced by *Pseudomonas fluorescens* ZX as biological fumigants against *Botrytis cinerea*. Microbiol. Res. 267, 127253. https://doi.org/10.1016/j.micres.2022.127253.